Physics and Imaging in Radiation Oncology 21 (2022) 48–53

Contents lists available at ScienceDirect

Physics and Imaging in Radiation Oncology

journal homepage: www.sciencedirect.com/journal/physics-and-imaging-in-radiation-oncology

Original Research Article

Comparison of visibility of iodinated hydrogel and gadolinium-modified hyaluronic acid spacer gels on computed tomography and onboard imaging

Vlora Riberdy [a,*], Ethan Ruiz [a], Nienke Hoekstra [b], Gerson Struik [c,d], Jean-Philippe Pignol [a]

[a] Department of Physics and Atmospheric Science, Dalhousie University, Halifax, NS, Canada
[b] Department of Radiation Oncology, Erasmus MC Cancer Institute, Rotterdam, The Netherlands
[c] Department of Surgery, Franciscus Gasthuis and Vlietland, Rotterdam, The Netherlands
[d] Department of Surgery, Erasmus MC Cancer Institute, Rotterdam, The Netherlands

ARTICLE INFO

Keywords:
Injectable spacer
Fiducial marker
Gadolinium contrast agent
Breast cancer radiotherapy

ABSTRACT

Background and purpose: In accelerated partial breast irradiation (APBI), accurate definition of the tumour bed is crucial to reduce the risk of local recurrence and the volume of healthy tissue irradiated. Recently, hydrogels have been proposed to improve visibility of the lumpectomy cavity for APBI. The aim of this study was to alter two commercially available hyaluronic acid (HA) gels, with gadopentenate dimeglumine (GD), a magnetic resonance imaging (MRI) contrast agent. We hypothesize that after injection in the surgical cavity, the mixtures will be visible with computed tomography (CT) for improved treatment planning, cone-beam CT (CBCT) for improved patient setup and planar kilovoltage (kV) x-ray for real-time tracking during treatment.
Materials and methods: In this *ex vivo* study, GD was mixed with the two HA gels, and 1 mL of each mixture was injected into fatty and muscular tissue of a pork phantom. Visibility with CT, CBCT and planar x-ray imaging was assessed. Contrast-to-noise ratios (CNR) were measured and compared to commercially available iodinated polyethylene glycol (PEG).
Results: The gel mixtures showed increased visibility over HA gels without GD. When comparing CNR of the gel mixtures to that of iodinated PEG on CT, there was a 4-fold increase in muscle for both mixtures and a 1.6-fold to 3.6-fold increase in fat, depending on the HA gel. Gel mixtures showed better visibility with planar kV imaging over iodinated PEG.
Conclusion: Addition of GD to HA gels increases visibility with CT, CBCT and planar x-ray imaging, indicating potential for improved delineation and positioning in APBI.

1. Introduction

Breast cancer is frequently diagnosed at an early stage because of the implementation of screening programs [1,2]. For these patients, breast-conserving surgery (BCS) followed by whole breast radiotherapy is the standard treatment and has demonstrated excellent survival rates and local control equivalent to mastectomy [3,4]. This treatment provides improved cosmetic outcomes and quality of life [5]. In accelerated partial breast irradiation (APBI), only the part of the breast surrounding the tumour bed is irradiated [6–8]. It reduces the amount of tissue irradiated and helps to reduce the amount of radiation scattered to the body, possibly providing a survival advantage in reducing the risk of death from secondary cancers [8]. For well selected low-risk patients, large multicenter randomized clinical trials have shown equivalent oncological outcomes for whole breast irradiation and APBI using brachytherapy [9–11], external 3D conformal radiotherapy [12,13], and intraoperative therapy [14,15].

APBI requires accurate target delineation for treatment planning, as well as a precise target localization during treatment since a geographical miss can lead to an increased risk of local recurrence and toxicity. The tumour bed is often easily identified on the planning computed tomography (CT) after superficial closure during BCS because of the development of a seroma. However, surgeons are increasingly performing full-thickness closure (FTC) of the excision cavity, as it results in a lower risk of post-surgical infection [16,17] and improved cosmesis [18]. The disadvantage of FTC is that it can hinder the

* Corresponding author at: Department of Medical Physics, 5820 University Ave., Halifax, NS B3H 1V7, Canada.
E-mail addresses: vlora.riberdy@nshealth.ca (V. Riberdy), ethan.ruiz@nshealth.ca (E. Ruiz), n.hoekstra@erasmusmc.nl (N. Hoekstra), G.Struik@Franciscus.nl (G. Struik), jean-philippe.pignol@dal.ca (J.-P. Pignol).

https://doi.org/10.1016/j.phro.2022.02.001
Received 30 July 2021; Received in revised form 10 February 2022; Accepted 11 February 2022

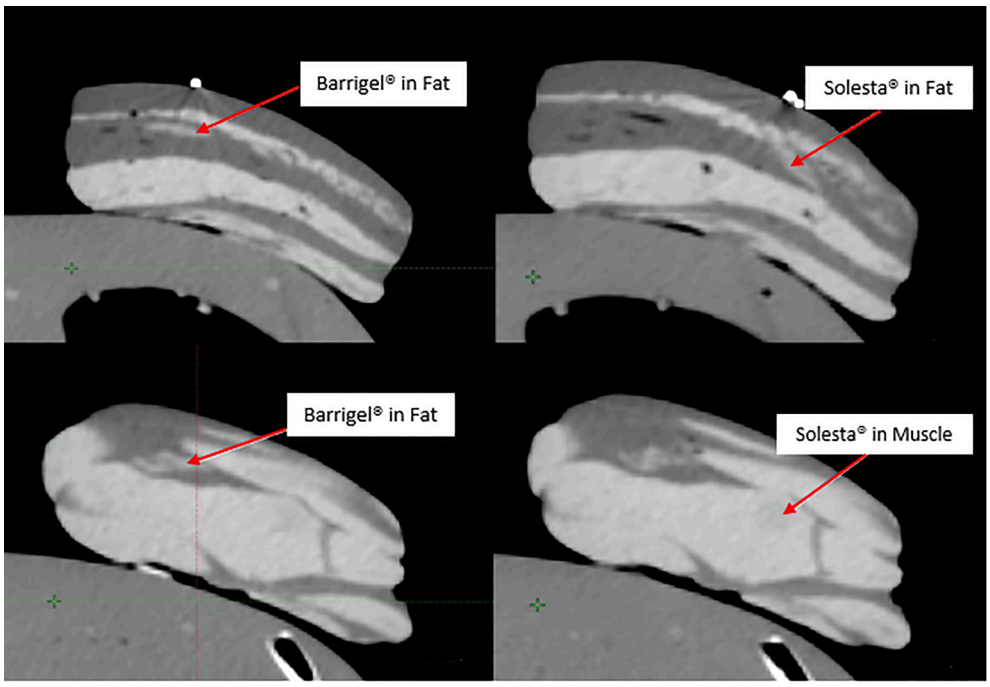

Fig. 1. CT slices (120 kVp) showing the injections of Barrigel® and Solesta® in fat (dark tissue) and muscle (lighter tissue). One injection of Barrigel® did not make it into the muscle and was injected into fat a second time.

visualization of the tumour bed on planning CT images. Seromas are often absent after FTC, making it difficult to contour the tumour bed. A study done by den Hartogh et al. [19] showed that localization of the tumour bed after FTC is imprecise on both CT and magnetic resonance imaging (MRI).

To increase the accuracy of target delineation, insertion of surgical clips in the tumour bed is recommended [20]. However, the target delineation based on clips has poor inter-observer agreement following oncoplastic surgery using FTC [19]. Due to the high atomic number of the clip materials, artifacts are often present in CT images, hindering accurate contouring. It has been reported that the positioning is not systematic, and often varying numbers of clips are used [21].

In recent years, injectable hydrogels have been used as spacers to separate critical structures from high dose areas, such as in prostate radiotherapy to spare the rectum [22]. Struik et al [23] showed that iodinated polyethylene glycol (PEG) injected at the time of lumpectomy resulted in high inter-observer agreement of APBI target definition. This iodinated PEG was well visible with CT, but not with planar kilovoltage (kV) imaging. There were also issues with dilution of the hydrogel over time due to seroma production.

An optimal gel marker would be clearly visible with CT and MRI for ease of treatment planning, as well as on kV cone beam CT (CBCT) and planar kV portal imaging for improved patient set-up. Visibility with planar kV imaging would be useful for motion tracking systems.Visibility with ultrasound is also a priority as the hydrogels could also be injected in the cavity under US guidance just before the planning CT to avoid dilution issues.

In this article we report the use of a high-Z gadolinium (Gd) contrast agent mixed with different injectable hyaluronic acid (HA) spacers. The purpose of this work was to evaluate two different commercially available HA spacers mixed with a gadolinium-based contrast agent, and compare CT, CBCT and planar kV imaging visibility in a pork phantom with iodinated PEG using contrast to noise ratio (CNR). The hypothesis was that the final product would enable improved treatment planning, patient set-up and target tracking compared to an existing iodinated PEG commercial product.

2. Materials and methods

2.1. Mixing HA gels with Magnevist®

Barrigel® (Palette Life Sciences, Santa Barbara, CA) is an injectable hyaluronic acid (HA) prostate spacer. Solesta® (Palette Life Sciences, Santa Barbara, CA) is an injectable gel which consists of dextranomer microspheres and stabilized HA in phosphate-buffered saline solution, used to treat fecal incontinence. Magnevist® (Bayer AG, Leverkusen, Germany) is a well-known MRI contrast agent. Its high atomic number makes it an ideal solution to mix with the HA gels to allow visibility with CT, CBCT and planar kV imaging.

The first step was to define the optimal concentration of Magnevist® to ensure visibility in planar kV imaging. We aimed to develop a Gd-modified HA gel with an attenuation twice that of a dense biological material typically seen on portal imaging. We chose a sphere of cortical bone with a radius of 1 cm as an attenuation reference. Knowing the density of cortical bone (1.92 g/cm^3), the fraction of calcium by weight (0.255), the density and Gd fraction of Magnevist® (0.0786 g/mL) and that the photoelectric effect is proportional to the atomic number cubed, we calculated the amount of Magnevist® needed.

The concentration of Magnevist® needed to have twice the attenuation of cortical bone was 35% (v/v), so 1.05 mL of Magnevist® was added to 2.95 mL of Barrigel® and Solesta® separately. However, this resulted in loss of HA-based gel consistency in both cases, rendering it useless. Further mixing trials showed that the maximum concentration of Magnevist® in Barrigel® and Solesta® without loss of consistency was 20% (v/v) and 33% (v/v), respectively. These concentrations were used for our experiments.

HA-based gels were removed from the syringe into a jar and the calculated volume of Magnevist® was added and mixed by hand. The mixture was then placed in another syringe for injections.

2.2. Phantom imaging

Barrigel® and Solesta® (1 cc) without added contrast were injected into fatty and muscular tissue of a pork phantom. The pork phantom was

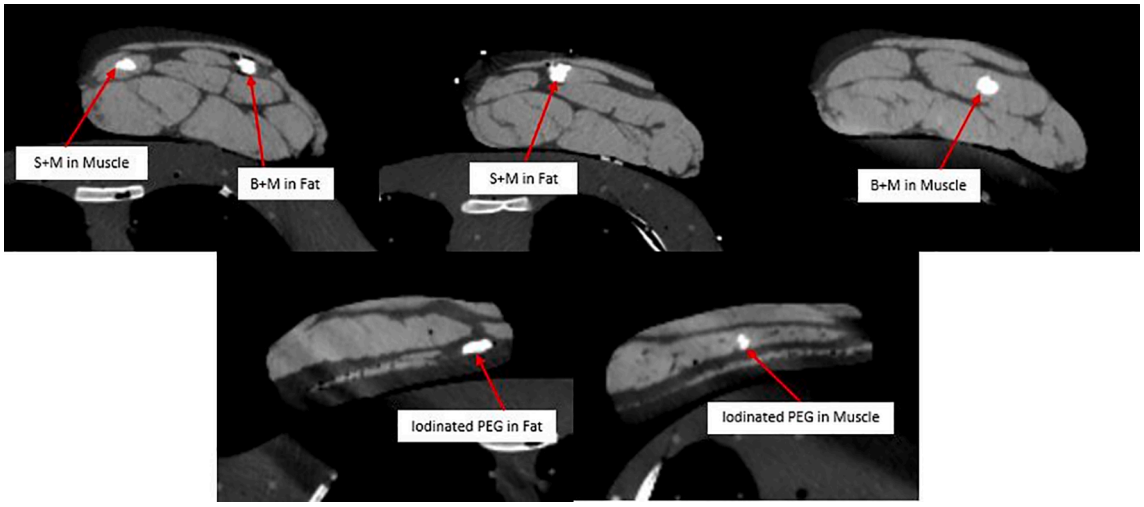

Fig. 2. Top row. CT slices (120 kVp) showing the injection of the gel mixtures in fat and muscle. B + M = Barrigel® + Magnevist®, S + M = Solesta® + Magnevist®. Bottom row: CT slices (120 kVp) showing the injections of iodinated PEG in fat and muscle.

taped on a Rando Phantom (RSD, Long Beach, CA) to mimic a human breast. CT-simulation (GE Healthcare, Boston, MA) was acquired with images of 1.25 mm and 2.5 mm slice thickness at 80, 120 and 140 kVp to determine the optimal parameters for future experiments. Metrics of success included visibility (identification against muscle or fat) and the presence of artifacts.

One cc of the two HA gel mixtures and of iodinated PEG was injected into fatty and muscular tissues of a second pork phantom. The phantom was first imaged with CT using a standard clinical breast protocol at 2.5 mm slice thickness and 120 kVp. CBCT was performed using a Truebeam 2.0 STx platform (Varian Medical Systems, Palo Alto, CA) with a source to imager distance of 150 cm. Two clinical protocols were used: a thorax protocol (125 kV, 270 mAs) that would typically be used in the clinic, and a head protocol (100 kV, 150 mAs) with a lower kV to possibly increase contrast. Planar kilovoltage imaging was performed using two standard clinical protocols: a thorax, arms up protocol (120 kV, 2.56 mAs) and a head protocol (70 kV, 5 mAs). The images were acquired laterally, both left–right and right-left. In a separate experiment aiming at improving the image contrast, the field size of the kV images was adjusted from 20 × 26 cm^2 to 9.5 × 14 cm^2 to encapsulate the pork phantom only and avoid scattered photon contamination from the Rando phantom.

2.3. Image quality analysis

The images were analyzed using standard CNR, which was defined as:

$$\mathrm{CNR} = \frac{|S_{ROI} - S_B|}{\sigma_B}$$

where S_{ROI} represents the average signal of a region-of-interest (ROI) in the image, S_B is the average signal within an ROI of the same size in the background material (fat or muscle), and σ_B is the standard deviation of the background ROI. S_{ROI} was calculated as the mean pixel value of a rectangular ROI within the gel volumes. All values were averaged over 5 slices, with various ROI sizes per slice, except for the images of Barrigel® and Solesta® without Magnevist®; for these experiments, 3 slices were used. CNR calculations were done using Matlab vR2019a (The MathWorks, Natick, MA).

Table 1
CNR (±standard deviation) of CT-sim images (120 kVp).

	Barrigel®	Solesta®	B + M	S + M	I-PEG
Muscle	–	3.3 ± 0.4	68.3 ± 15.7	69.4 ± 14.7	15.6 ± 3.2
Fat	10.6 ± 5.4	8.2 ± 5.8	43.4 ± 13.8	100.9 ± 21.7	27.7 ± 11.9

3. Results

3.1. CT Imaging and CNR

Visibility of both gels was better in fat than in muscle (Fig. 1). Out of note, one injection of Barrigel® missed the muscle and was injected into fat a second time. The best quality images were obtained using the standard 120 kVp and 2.5 mm slice thickness breast protocol. Thinner slices and lower energy resulted in increased artifacts. All future CT scans were performed with 2.5 mm slice thickness and 120 kVp. For the CBCT scans, 100 and 125 kVp were used.

Fig. 2 shows that the addition of Magnevist® increased visibility of the gels in fatty and muscular tissue of the pork phantoms.. CBCT images of these phantoms can be found in the Supplementary Material. No artifacts were present in these CT or CBCT images.

Table 1 shows the calculated CNR (mean ± standard deviation) in the CT images for all injections in fatty and muscular tissue. Comparing the Barrigel® + Magnivist® mixture with Barrigel® alone, there was an increase of the CNR by a factor of 5 in muscle and 4 in fat. For Solesta®, there was an increase in the CNR by a factor of 20 in muscle and 12 in fat after the addition of Magnevist®. The CNR increased 4-fold when comparing both gel mixtures to the iodinated PEG in muscular tissue. In fatty tissue, the increase was 1.6-fold for Barrigel® + Magnivist® and 3.6-fold for Solesta® + Magnevist®.

These CNR measurements were repeated for the CBCT images. The resulting CNR values can be found in the Supplementary Material. Barrigel® and Solesta® without Magnevist® were not visible with CBCT imaging, both at 100 kVp and 125 kVp. For the thorax protocol (125 kVp), the CNR of the gel mixtures increased 2-fold compared to the iodinated PEG in muscle. In fat there was no relevant change. For the head protocol (100 kV), the CNR of the Barrigel® + Magnivist® mixture increased 4-fold and the CNR of the Solesta® + Magnevist® mixture increased 5-fold compared to the iodinated PEG in muscle. In fat, the CNR of the Barrigel® + Magnivist® mixture increased 2.6-fold and that of the Solesta® + Magnevist® mixture increased 4.4-fold.

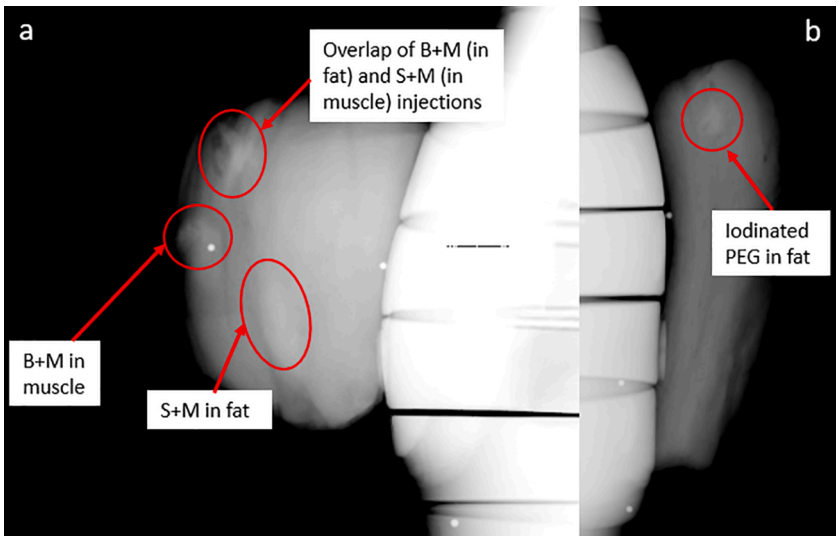

Fig. 3. (a) Planar kV image (70 kVp) of a pork phantom injected with the gel mixtures. (b) Planar kV image (70 kV) of a pork phantom injected with iodinated PEG. Visible injections circled in red.

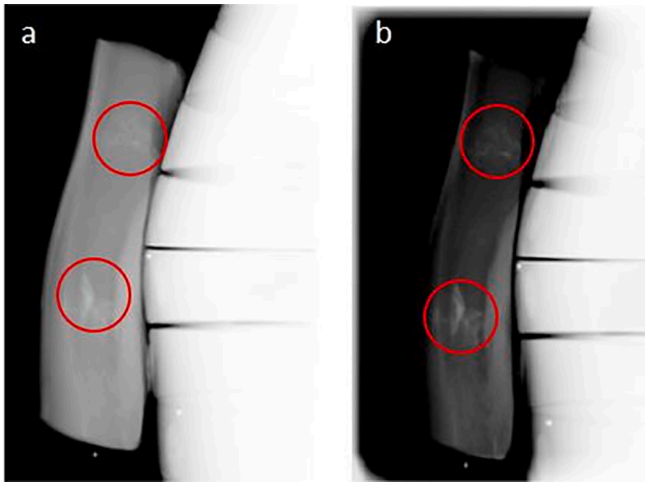

Fig. 4. Planar kV images (70 kVp) of Gd-modified HA gels injected into a pork phantom. (a) Field Size of 20 × 26 cm^2. (b) Field size of 9.5 × 14 cm^2. The top injection is B + M and the bottom injection is S + M (same window width and level).

3.2. Planar kV Imaging

The two Gd-modified HA gels were both visible in planar kV imaging after being injected into fatty and muscular tissue (Fig. 3a). The Solesta® + Magnevist® injection in fat was difficult to find. Reconstructed sagittal CT slices helped with locating this injection (Supplementary Material Fig. 2). In contrast, only one injection of the iodinated PEG was visible (Fig. 3b). These results were also seen with the other imaging protocol used. The visibility of the injected Gd-modified HA gels was slightly increased using collimation, as can be seen in Fig. 4.

4. Discussion

This study demonstrates that Magnevist® added to HA-based gels injected into a biological tissue phantom provides immediate visibility and increased CNR in CT, CBCT and planar kV imaging compared to previously studied iodinated PEG. The use of HA-based gels containing Magnevist® is promising to further improve radiotherapy target definition. Visibility with CT and CBCT is similar for the iodinated PEG and the HA-gel mixtures used in this study, however, visibility with planar kV imaging is superior for the HA-gel mixtures.

The use of iodinated PEG injected into the surgical cavity has been shown to improve the interobserver agreement in breast radiotherapy target definition, however there were issues with dilution due to seroma formation [23]. HA gels have been used as spacers in radiotherapy [22] and have recently been studied as a tumour bed marker in BCS [24]. Both these studies showed that interobserver variability in delineation increased with the use of injected gels. The visibility of these gels on kV imaging was not studied. The gadolinium modified HA gels in this study could also improve delineation while aiding with patient setup and target tracking due to visibility in planar kV imaging.

Currently, target delineation for planning and patient positioning for breast cancer patients is mostly done using surgical clips. The gel mixtures offer several advantages over surgical clips. Surgical clips are made of either titanium (Z = 22) or tantalum (Z = 73). Tantalum is better seen on portal imaging, but it causes streak artifacts on CT images, making the contouring of the seroma more challenging [25]. Gadolinium also has a high atomic number (Z = 64), but dispersing it in a gel may prevent the occurrence of artifacts, depending on the concentration and x-ray energy. Fig. 2 shows no artifacts due to presence of Magnevist® at the current concentration. The HA-gel mixtures are located within the entire tumour bed, whereas clips are pushed into the walls and mark them at a limited number of locations and may not accurately represent the original tumour site [26]. Using the HA-gel mixtures may provide the radiation oncologist with more information on the tumour bed location and extent, resulting in less variability in delineation. Movement of surgical clips between surgery and treatment is a possibility, requiring increased planning target volumes [27].

Both Barrigel® and Solesta® provided increased CNR over the iodinated PEG. Gadolinium has a higher atomic number than iodine (Z = 53) offering a major advantage in x-ray absorption with kV imaging, as the photoelectric effect is dominant in this energy range and is proportional to Z^3. Since the Solesta® mixture had a higher concentration of Magnevist®, its CNR was higher than that of the Barrigel® mixture for CT and CBCT. The CBCT head protocol utilizes a lower kV than the thorax protocol (100 kV vs. 125 kV). The differences in CNR between the Gd-modified HA gels and iodinated PEG were larger with the head protocol. With lower kV, contrast can be increased due to greater differences in attenuation between materials.

Fig. 4 shows that reducing the field size with planar kV imaging increases the contrast and visibility of the gel mixtures. This can be explained by the fact that decreasing the field size reduces the amount of

scattered radiation reaching the detector. An added benefit is that it reduces the dose to the patient. When imaging laterally, contralateral breast tissue can obstruct visibility of the gel mixtures. In this case, reducing the field size can help to increase contrast. The field size can be reduced to encompass the breast only or only the tumour bed inside the breast. The field sizes used in this study are realistic values that could be used in the clinic, depending on patient size.

Before implementing the use of HA-gel mixtures in clinical practice, injection parameters need to be optimized. In this study, 1 cc of gel was injected in each case. We have not performed tests varying the injected volume and it should be optimized to minimize expansion of the target volume but ensure visibility of the entire cavity. Also, the CNR may be proportional to the shape of the injection. The CNR is higher when the HA-gel mixture has a compact shape rather than spread out over a larger volume. In this study, the injections were performed without ultrasound guidance, but in the clinic, ultrasound will be used to guide post-operative injections. Pork phantoms don't mimic the exact tissue types in a breast. Patients may have several breast densities that can impact the visibility of the injections. The gel will be injected in a cavity surrounded by fatty or fibroglandular tissues. This will help to guide and improve the injection shape.

The visibility of the HA-gel mixtures inside the tumour bed on planar kV imaging can enable real-time tracking during treatment. The Synchrony® Respiratory Tracking System for the Cyberknife® (Accuray Inc, Sunnyvale, CA) tracks and corrects for patient motion during treatment with repeated orthogonal planar kV images of internal markers and an external breathing signal [28]. With increased visibility after an injection of the Gd-modified HA gel, this system may be able to accurately track the target volume without the need to implant gold fiducials. This would reduce treatment burden for early-stage breast cancer patients treated with partial breast irradiation using Cyberknife®.

This study only analyzed the change in CNR immediately after injection of the gel mixtures. Ideally, visibility of the gel mixtures should remain constant for the entirety of the treatment (up to 6–8 weeks) and have good US visibility. The contrast agent needs to be retained within the gel for this period. Blood flow in the vicinity of the injection site may carry Magnevist® out of the gel, decreasing visibility over time. Future studies will need to observe the retention of the contrast agent, most likely through animal studies. The advantage of animal studies would be to have a pharmacokinetic model with physiological exchange between blood and tissue including potential enzymatic degradation of the HA gels. The HA-based gels have been shown to remain in the body for up to 12 months when used for prostate rectum separation [29]. This indicates that the HA-based gels used in this study may be present in the breast at the time follow up imaging. It is not known whether this will affect the accuracy of the diagnosis of a local recurrence early during follow up. Future studies should include this effect. As the gel disappears from the body after 12 months, no problems with long-term follow up imaging are expected.

In conclusion, this study shows that mixing Magnevist® with the HA-based gels improves visibility of the gels and results in increased CNR in CT and CBCT images compared to iodinated PEG. The images are free from artifacts and the injections are visible with planar kV imaging. The use of HA-gel mixtures may improve the accuracy of target delineation and patient positioning and enable real-time tracking of the tumour bed during irradiation.

Declaration of Competing Interest

The authors declare the following financial interests/personal relationships which may be considered as potential competing interests: VR is a trainee in the Cancer Research Training Program of the Beatrice Hunter Cancer Research Institute, with funds provided by the Dalhousie Medical Research Foundation Rosetti Studentship. This source of funding did not have any involvement in study design, data collection and analysis, report writing and submission. This work is also partially funded by Palette Life Sciences. This source of funding did not have any involvement in study design, data collection and analysis, report writing and submission.

Acknowledgments

VR is a trainee in the Cancer Research Training Program of the Beatrice Hunter Cancer Research Institute, with funds provided by the Dalhousie Medical Research Foundation Rosetti Studentship. This work is also partially funded by Palette Life Sciences.

Appendix A. Supplementary data

Supplementary data to this article can be found online at https://doi.org/10.1016/j.phro.2022.02.001.

References

[1] SEER Database. Cancer stat facts: Female breast cancer, https://seer.cancer.gov/statfacts/html/breast.html. [Accessed September 2019].
[2] Peto R, Boreham J, Clarke M, Davies C, Beral V. UK and USA breast cancer deaths down 25% in year 2000 at ages 20–69 years. Lancet 2000;355:1822. https://doi.org/10.1016/S0140-6736(00)02277-7.
[3] Darby S, McGale P, Correa C, Taylor C, Arriagada R, Clarke M, et al. Effect of radiotherapy after breast-conserving surgery on 10-year recurrence and 15-year breast cancer death: meta-analysis of individual patient data for 10 801 women in 17 randomized trials. Lancet 2011;378:1707–16. https://doi.org/10.1016/S0140-6736(11)61629-2.
[4] Fisher B, Anderson S, Bryant J, Margolese RG, Deutsch M, Fisher ER, et al. 20-year follow-up of a randomized trial comparing total mastectomy, lumpectomy, and lumpectomy plus irradiation for the treatment of invasive breast cancer. N Engl J Med. 2002;347:1233–41. https://doi.org/10.1056/NEJMoa022152.
[5] Kim MK, Kim T, Moon HG, Jin US, Kim K, Kim J, et al. Effect of cosmetic outcome on quality of life after breast cancer surgery. Eur J Surg Oncol. 2015;41:426–32. https://doi.org/10.1016/j.ejso.2014.12.002.
[6] Polgár C, van Limbergen E, Pötter R, Kovács G, Polo A, Lyczek J, et al. Patient selection for accelerated partial-breast irradiation (APBI) after breast-conserving surgery: Recommendations of the Groupe Européen de Curiethérapie -European Society for Therapeutic Radiology and Oncology (GEC-ESTRO) breast cancer working group based on clinical evidence (2009). Radiother Oncol. 2010;94:264–73. https://doi.org/10.1016/j.radonc.2010.01.014.
[7] Shaitelman SF, Lin HY, Smith BD, Shen Y, Bedrosian I, Marsh GD, et al. Practical implications of the publication of consensus guidelines by the American Society for Radiation Oncology: accelerated partial breast irradiation and the National Cancer Data Base. Int J Radiat Oncol Biol Phys. 2016;94:338–48. https://doi.org/10.1016/j.ijrobp.2015.10.059.
[8] Correa C, Harris EE, Leonardi MC, Smith BD, Taghian AG, Thompson AM, et al. Accelerated partial breast irradiation: Executive summary for the update of an ASTRO evidence-based consensus statement. Pract Radiat Oncol. 2017;7:73–9. https://doi.org/10.1016/j.prro.2016.09.007.
[9] Pignol JP, Caudrelier JM, Crook J, McCann C, Truong P, Verkooijen HA. Report on the clinical outcomes of permanent breast seed implant for early-stage breast cancers. Int J Radiat Oncol Biol Phys. 2015;93:614–21. https://doi.org/10.1016/j.ijrobp.2015.07.2266.
[10] White J, Winter K, Kuske RR, Bolton JS, Arthur DW, Scroggins T, et al. Long-term cancer outcomes from study NRG Oncology/RTOG 9517: A phase 2 study of accelerated partial breast irradiation with multicatheter brachytherapy after lumpectomy for early-stage breast cancer. Int J Radiat Oncol Biol Phys. 2016;95:1460–5. https://doi.org/10.1016/j.ijrobp.2016.03.037.
[11] Polgár C, Ott OJ, Hildebrandt G, Kauer-Darner D, Knauerhase H, Major T, et al. Late side-effects and cosmetic results of accelerated partial breast irradiation with interstitial brachytherapy versus whole-breast irradiation after breast-conserving surgery for low-risk invasive and in-situ carcinoma of the female breast: 5-year results of a randomized, controlled, phase 3 trial. Lancet Oncol. 2017;18:259–68. https://doi.org/10.1016/S1470-2045(17)30011-6.
[12] Vicini F, Winter K, Straube W, Wong J, Pass H, Rabinovitch R, et al. A phase I/II trial to evaluate three-dimensional conformal radiation therapy confined to the region of the lumpectomy cavity for stage I/II breast carcinoma: Initial report of feasibility and reproducibility of radiation therapy oncology group (RTOG) study 0319. Int J Radiat Oncol Biol Phys. 2005;63:1531–7. https://doi.org/10.1016/j.ijrobp.2005.06.024.
[13] Coles CE, Griffin CL, Kirby AM, Titley J, Agrawal RK, Alhasso A, et al. Partial-breast radiotherapy after breast conservation surgery for patients with early breast cancer (UK IMPROT LOW trial): 5-year results from a multicentre, randomized, controlled, phase 3, non-inferiority trial. Lancet 2017;390:1048–60. https://doi.org/10.1016/S0140-6736(17)31145-5.
[14] Vaidya JS, Bulsara M, Baum M, Wenz F, Massarut S, Pigorsch S, et al. Long term survival and local control outcomes from singla dose targeted intraoperative radiotherapy during lumpectomy (TARGIT-IORT) for early breast cancer: TARGIT-A randomized clinical trial. BMJ 2020;370:m2836. https://doi.org/10.1136/bmj.m2836.

[15] Indelicato D, Grobmyer SR, Newlin H, Morris CG, Haigh LS, Copeland EM, et al. Association between operative closures type and acute infection, local recurrence, and disease surveillance in patients undergoing breast conserving therapy for early-stage breast cancer. Surgery. 2007;141:645–53. https://doi.org/10.1016/j.surg.2006.12.011.

[16] Veronesi U, Orecchia R, Maisonneuve P, Viale G, Rotmensz N, Sangalli C, et al. Intraoperative radiotherapy versus external radiotherapy for early breast cancer (ELIOT): a randomized controlled equivalence trial. Lancet Oncol. 2013;14:1269–77. https://doi.org/10.1016/S1470-2045(13)70497-2.

[17] Mukesh B, Barnett G, Cumming J, Wilkinson JS, Moody AM, Wilson C, et al. Association of breast tumour bed seroma with post-operative complications and normal tissue toxicity: results from the Cambridge Breast IMRT trial. Eur J Surg Oncol. 2012;38:918–24. https://doi.org/10.1016/j.ejso.2012.05.008.

[18] Clough KB, Kaufman GJ, Nos C, Buccimazza I, Sarfati IM. Improving breast cancer surgery: a classification and quadrant per quadrant atlas for oncoplastic surgery. Ann Surg Oncol 2010;17:1375–91. https://doi.org/10.1245/s10434-009-0792-y.

[19] den Hartogh MD, van den Bongard D, Davidson MTM, Kotte ANTJ, Verkooijen HM, Philippens MEP, et al. Full-thickness closure in breast-conserving surgery: the impact on radiotherapy target definition for boost and partial breast irradiation. A multimodality image evaluation. Ann Surg Oncol. 2014;21:3774–9. https://doi.org/10.1245/s10434-014-3801-8.

[20] Coles CE, Wilson CB, Cumming J, Benson JR, Forouhi P, Wilkinson JS, et al. Titanium clip placement to allow accurate tumour bed localization following breast conserving surgery – audit on behalf of the IMPORT Trial Management Group. Eur J Surg Oncol. 2009;35:578–82. https://doi.org/10.1016/j.ejso.2008.09.005.

[21] Azu M, Goyal S, Patel U, Haffty B, Kearney T. Has placement of surgical clips in the lumpectomy bed fallen out of favour? Ann Surg Oncol. 2011;18:1529–32. https://doi.org/10.1245/s10434-011-1672-9.

[22] Hamstra DA, Mariados N, Sylvester J, Shah D, Karsh L, Hudes R, et al. Continued benefit to rectal separation for prostate radiation therapy: final results of a phase III trial. Int J Radiat Oncol Biol Phys. 2017;97:976–85. https://doi.org/10.1016/j.ijrobp.2016.12.024.

[23] Struik GM, Hoekstra N, Klem TM, Ghandi A, Verduijn GM, Swaak-Kragten AT, et al. Injection of radiopaque hydrogel at time of lumpectomy improves the target definition for adjuvant radiotherapy. Radiother Oncol. 2019;131:8–13. https://doi.org/10.1016/j.radonc.2018.11.003.

[24] Wiercińska J, Winiecki J, Wronczewska A, Lebioda A, Pławski K, Rhone P, et al. The use of hyaluronic acid hydrogel as a tumour bed marker in breast-conserving therapy. Radiother Oncol. 2020;152:8–13. https://doi.org/10.1016/j.radonc.2020.07.041.

[25] Thomas CW, Nichol AM, Park JE, Hui JF, Giddings AA, Grahame S, et al. An anthropomorphic phantom study of visualisation of surgical clips for partial breast irradiation (PBI) setup verification. Radiother Oncol. 2009;90:56–9. https://doi.org/10.1016/j.radonc.2008.03.011.

[26] Yang Z, Chen J, Hu W, Pan Z, Cai G, Yu X, et al. Planning the breast boost: How accurately do surgical clips represent the CT seroma? Radiother Oncol. 2010;97:530–4. https://doi.org/10.1016/j.radonc.2010.09.007.

[27] Hoekstra N, Habraken S, Swaak - Kragten A, Pignol JP, Hoogeman M. Fiducial marker motion relative to the tumor bed has a significant impact on PTV margins in partial breast irradiation. Radiother Oncol. 2021;163:1–6. https://doi.org/10.1016/j.radonc.2021.07.020.

[28] Hoogeman M, Prévost t JB, Nuyttens J, Pöll J, Levendag P, Heijmen B. Clinical accuracy of the respiratory tumor tracking system of the Cyberknife: assessment by analysis of log files. Int J Radiat Oncol Biol Phys 2009;74:293–303. https://doi.org/10.1016/j.ijrobp.2008.12.041.

[29] Mok G, Benz E, Vallee JP, Miralbell R, Zilli T. Optimization of radiation therapy techniques for prostate cancer with prostate-rectum spacers: a systematic review. Int J Radiat Oncol Biol Phys. 2014;90:278–2788. https://doi.org/10.1016/j.ijrobp.2014.06.044.